RF safety of the combination of a ^{31}P Tx/Rx endorectal coil and a ^{1}H Tx/Rx body array for ^{31}P MRSI of the prostate at 7T

Andreas K. Bitz[1,2], Thiele Kobus[3], Tom W. J. Scheenen[1,3], and Mark E. Ladd[1,2]

[1]*Erwin L. Hahn Institute for Magnetic Resonance Imaging, University Duisburg-Essen, Essen, Germany,* [2]*Department of Diagnostic and Interventional Radiology and Neuroradiology, University Hospital Essen, Essen, Germany,* [3]*Department of Radiology, Radboud University Nijmegen Medical Centre, Nijmegen, Netherlands*

Introduction: ^{31}P MR spectroscopic imaging (^{31}P MRSI) of the human prostate at 7T provides information about phosphorylated metabolites that could be used for prostate cancer characterization [1]. To relate the metabolic information to anatomical location, a ^{31}P Tx/Rx endorectal coil (ERC) was combined with an eight-channel ^{1}H Tx/Rx body array coil [1]. To test compliance with respect to RF safety [2], RF coupling between the body array and the ERC needs to be investigated even though both coils operate at different Larmor frequencies. RF coupling could lead to unpredictable flip angle distributions, increased local SAR, and elevation of the tissue temperature. Safety testing for the body array coil can be performed based on SAR limits. For the ERC, it has to be validated that the 10g-averaged SAR (SAR_{10g}) does not underestimate the RF exposure due to the close proximity of RF-radiating structures to the human tissue, e.g. by assessing the temperature distribution in the human body. The compliance test for the coil combination was performed by numerical simulation (CST Studio Suite 2011, Darmstadt, Germany) as well as by measurements *in vivo*. All measurements were performed on a 7T whole body MR system (Magnetom 7T, Siemens, Erlangen, Germany).

Materials & Methods: For the ^{31}P ERC the housing and conductors of an inflatable 3T ERC (Medrad, USA) were adapted and tuned/matched to 50 Ω at 120.3 MHz [1]. The ^{1}H body array coil for imaging consists of eight meander stripline elements and can be flexibly adjusted to the volunteer's contour [3]. MR imaging was performed with an RF shimming system [4] including RF power monitoring [5]. From numerical computations of the RF field produced by the ERC, the maximum input power to comply with the SAR_{10g} limit of 10 W/kg was determined. A detailed model of the coil including the feeding coaxial RF cable and the surrounding tissues was developed for this purpose (Fig. 1a). To validate that the SAR_{10g} does not underestimate the RF exposure, thermal simulations were performed by use of Pennes' bio-heat transfer equation (BHE) [6]. Next, the input power (P_{in}) at which the local temperature limit of 39°C [2] was reached after a scan duration of 15 minutes was derived. To take into account the influence on the RF-induced temperature of the active thermal regulation, which is not included in the BHE, temperature measurements were carried out *in vivo* by fiber optic temperature sensors positioned at the previously determined location of highest temperature. The input power which resulted in 1 °C temperature increase during 15 minute MRSI was determined. The temperature increase of 1°C was chosen to assure that the absolute temperature limit of 39 °C is not exceeded *in vivo*, independent of the thermal regulation of the individual volunteer. The coupling of the array coil with the ERC was assessed by simulations with a heterogeneous 70 kg male body model [7]. The applied excitation mode of the body array was an RF shim with maximal $|B_1^+|$ in the prostate. Simulations were performed with and without the ERC. At both transmit frequencies, the coupling of the coil ports was monitored and it was evaluated whether relevant elevations of B_1^+ and SAR occurred due to interactions between the coils. The SAR findings were additionally confirmed by thermal simulations in the body model. Finally, the maximum permissible input power of the body array coil was determined based on the limit for the localized SAR.

Results: The RF simulations for the ERC showed that at an input power of 0.95 W the SAR_{10g} limit was reached (Fig. 1b), whereas thermal simulations showed that a power of 1.3 W would be allowed without exceeding a local temperature of 39°C after a scan duration of 15 min (Fig. 1c). In the *in vivo* temperature measurements, 1.9 W applied for the duration of 15 minutes resulted in a temperature increase of just below 1°C (Fig. 1d). The simulations predicted that the excitation ports of both coils at both operating frequencies were well decoupled by at least -50 dB. Corresponding measurements showed an average coupling of -71 dB at 120.25 MHz and -70 dB at 297.05 MHz, demonstrating excellent decoupling. During ^{1}H imaging with the body array, no significant B_1^+ distortions and no relevant SAR elevation due to the ^{31}P ERC located in the rectum were visible (Fig. 2a-d). The highest SAR was located close to the individual elements of the array coil near the body surface, and the maximum SAR_{10g} using the prostate RF shim settings was close to the upper left coil element. This was further supported by temperature simulations, which also showed no difference in temperature distribution with or without the ERC after a 15 minute measurement (Fig. 2e-f). The maximum permissible input power of the body array coil at which the safety limit for the localized SAR of 10 W/kg was not exceeded was 33 W.

Conclusion: Simulations and measurements confirmed that the effect of the ERC on the B_1^+ and SAR distribution of the eight-channel array coil is negligible. Thus, it can be concluded that the presence of the ^{31}P ERC does not influence the SAR distribution of the ^{1}H body array coil. Moreover, due to the negligible coupling, the simulation model for the ERC does not need to take into account the complete body model or the body array coil. Whereas the maximum permissible input power for the array coil was derived from the SAR limit, the input power for the ERC was derived from *in vivo* temperature measurements, since the location of the maximum temperature increase was accessible by a fiber optic sensor inserted together with the ERC. Based on the *in vivo* temperature, a higher input power was allowed because heat can be dissipated by blood flow through the tissue. Interestingly, the localized SAR overestimates the RF exposure by the ERC for the considered configuration.

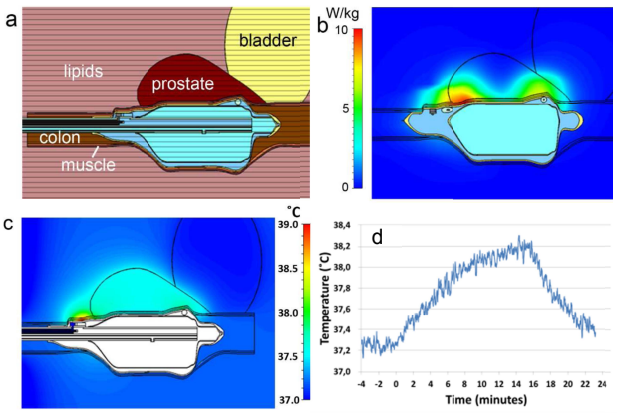

Figure 1: Safety validation of the ^{31}P endorectal coil. (a) Simulation model for the ERC and surrounding tissues. (b) Calculated SAR_{10g} at P_{in} = 0.95 W. (c) Calculated temperature distribution at P_{in} = 1.3 W. (d) Temperature measured *in vivo* at P_{in} = 1.9 W.

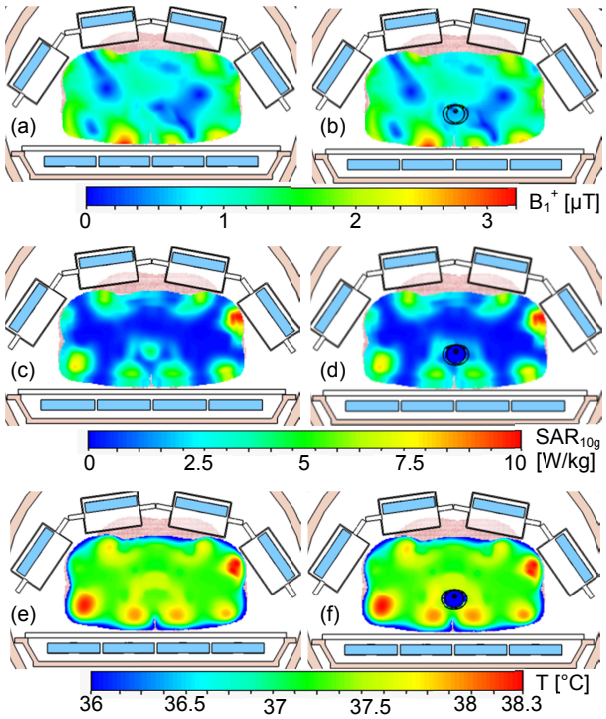

Figure 2: Simulations for body model and ^{1}H body array without (a,c,e) and with (b,d,f) ^{31}P ERC at P_{in} = 33 W. (a,b) B_1^+ distribution, (c,d) 10g-averaged SAR, (e,f) temperature distribution.

References: [1] Kobus et al. Proc. ISMRM 19 (2011), 3057. [2] IEC International standard 60601-2-33; 2010. [3] Orzada et al. Proc. ISMRM 17 (2009), 2999. [4] Bitz et al., Proc. ISMRM 17 (2009), 4767. [5] Brote et.al., Proc. ISMRM 17 (2009), 4788. [6] Pennes HH. J Appl Physiol 1998;85(1):5-34. [7] Christ et al. Physics Med Biol 2010;55(2):N23-38.